Proceedings of the ASME 2024
Verification, Validation and Uncertainty Quantification Symposium
VVUQ2024
May 15-17, 2024, College Station, TX, USA

VVUQ2024-132617

FINITE ELEMENT MODEL VALIDATION OF CRYOGENIC DOT-113 TANK CAR SIDE IMPACT TESTS

Shaun Eshraghi, Michael Carolan, Benjamin Perlman,
Volpe National Transportation Systems Center
U.S. Department of Transportation
Cambridge, Massachusetts, USA

Francisco González III
Federal Railroad Administration
U.S. Department of Transportation
Washington, DC, USA

ABSTRACT

The U.S. Department of Transportation's (USDOT's) Federal Railroad Administration (FRA) has sponsored a series of four full-scale side impact tests on specification DOT-113 railroad tank cars. A DOT-113 is a specially designed tank car intended to transport cryogenic liquid commodities. For each side impact test, researchers at the USDOT's Volpe National Transportation Systems Center (Volpe Center) created a pre-test finite element (FE) model to estimate the overall force-time response of the impactor, puncture/non-puncture outcomes of the impacted tank car, global motions of the tank car, internal pressures within the tank car, and the energy absorbed by the tank car during the impact. While researchers have previously compared FE model results to test measurements for tank car side impact tests, there are currently no formal guidelines on what measurable level of agreement is an acceptable demonstration of FE model validation. This paper presents FE model validation of DOT-113 and DOT-113 surrogate side impact tests using a publicly available software named Correlation and Analysis Plus (CORA) [1] which was originally developed for automotive crashworthiness using models of anthropomorphic test devices, i.e., crash test dummies.

The authors have previously presented FE model validation frameworks for impact simulations [2] and demonstrated FE model validation for non-cryogenic tank car side impacts [3] using CORA and another software called Roadside Verification and Validation Program (RSVVP) [4]. The authors have decided to use CORA in this paper because its validation metrics and rating procedures are included in an ISO technical specification for road vehicles (ISO/TS 18571:2014) [5]. Conversely, RSVVP is not incorporated in a US or international specification.

The results indicate that CORA can be directly applied to tank car side impact model results using the procedures in ISO/TS 18571:2014 when the model does not self-terminate due to puncture. The FE models achieved excellent and good CORA scores for cases without puncture of the tank car. However, early termination of the FE model due to puncture disrupted the automated post-processing of the model results for the two tests that produced a puncture outcome. Further consideration is necessary to develop guidelines that can produce useful validation scores for FE models that include a puncture outcome.

1. INTRODUCTION

In recent years, significant research has been conducted to analyze and improve the impact behavior and puncture resistance of railroad tank cars used in the transportation of hazardous materials. Ultimately, the results of this research can be used by the USDOT in the US and Transport Canada (TC) in Canada to establish performance-based testing requirements and to develop methods to evaluate the crashworthiness and structural integrity of different tank car designs when subjected to a standardized side impact scenario. A performance-based requirement for tank car head (i.e., the rounded ends of the car) impact protection has already been defined within the current regulations [5], and an optional performance-based requirement for tank car side impact resistance is applicable to specification DOT-117P tank cars [6].

Since 2007, the FRA has sponsored a series of side impact tests of tank cars of various designs, using a standardized impact test setup as shown in Figure 1. The standardized side impact test setup constrains the tank car's motion by supporting the car against a rigid barrier. This creates a severe impact condition for the tank car's shell, as the kinetic energy (KE) of the initially moving ram car must be dissipated almost entirely through deformation of the struck tank car. Since the mass of the impacting ram car was approximately the same in all the tests, impact speed and initial KE are interchangeable measures of the impact conditions in each test.

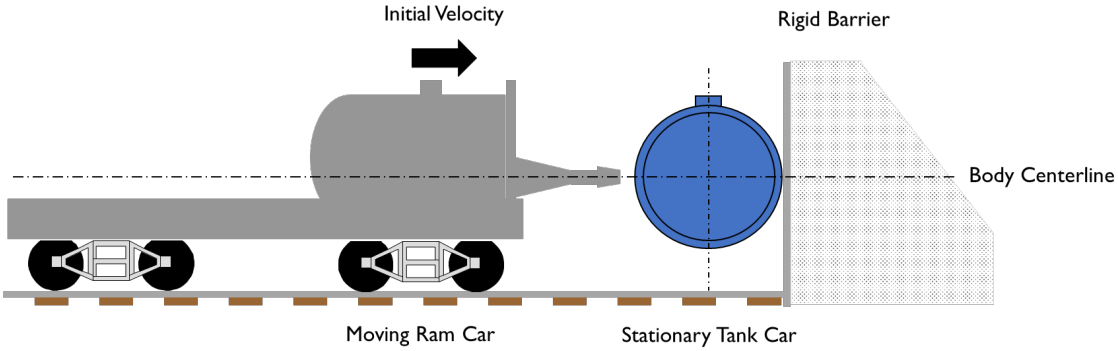

Figure 1. Schematic of Standardized Side Impact

One of the key outcomes of each test is whether, under the defined impact conditions, the tank car was punctured or resisted the impact without puncturing. If puncture occurs, a key measurement from the test is the puncture energy calculated by integrating impactor force versus impactor travel up to the point of puncture. A table summarizing the four most recent side impact tests is shown in Table 1. These side impact tests have involved testing of DOT-113 and DOT-113 surrogate tank cars filled with either water/air or liquid/gaseous nitrogen (LN2/GN2). The DOT-113 surrogates described in this paper included the features of a DOT-113 tank car essential to evaluating their impact response (e.g., typical tank materials, lading, thicknesses, and diameters) but did not include features such as couplers, brake rigging, and other tank car specific features that would not affect the impact response. Similarly, LN2 was used as a surrogate cryogenic lading in place of cryogenic liquid hydrocarbons such as methane and ethylene because it was more inert and therefore safer for testing that was expected to produce a puncture and release of the cryogenic lading.

Table 1. Summary of Class DOT-113 Tank Car Side Impact Tests

Test	Test Date	Spec.	Lading	Impact Speed	Puncture Energy	Ref.
#	*MM/YYYY*	-	-	*mph*	*10^6 ft-lbf*	-
10	11/2019	DOT-113C120W	Water	16.7	2.1	[7]
11	06/2020	DOT-113 Surrogate	Water	17.3	-	[8]
12	07/2021	DOT-113 Surrogate	LN2	18.3	-	[9]
13	05/2022	DOT-113C120W9	LN2	22.1	4.3	[10]

FE modeling is used in conjunction with each test to plan for the impact conditions, estimate the tank's response under those conditions, evaluate alternative impact conditions, and extrapolate from the test conditions to other conditions of interest. A primary purpose for pre-test modeling is to estimate the target impact speed for an upcoming test, and how that speed may relate to a threshold puncture speed. The threshold puncture speed can be thought of as the maximum speed at which the tank car can be impacted under the prescribed conditions without resulting in a tear to its shell that would allow its lading to escape. Puncture speed is a useful metric for comparing the relative performance of different tank car designs under similar impact conditions as the goal of the research program is to improve the performance of tank cars involved in incidents, including reducing the likelihood of a release of hazardous materials.

Ideally, the pre-test FE model can predict all the responses that are measured or observed during the test. In practice, some differences between the FE results and the test measurements are expected. Additionally, based on the actual impact conditions (e.g., measured impact speed, outage volume, outage pressure), it is usually necessary to make some adjustment to the pre-test model after the test to be able to simulate the actual test conditions, creating a post-test model. Depending on the nature of the changes made to the model, these changes may be considered calibration or tuning of the side impact model, where the intent is to adjust the physical modeling parameters in the model to better match the test data. Alternatively, the changes may simply be adjustments to the pre-test model to better match the actual test conditions [2].

Given that there will be differences between the test measurements and corresponding results from an FE model, it is valuable to develop targets for comparisons to be made between the test measurements and FE results to be used to validate that the model is producing physically-realistic results for the system being modeled [2]. This is especially important if an FE model is intended to be used to simulate conditions beyond what was tested, as there will not be corresponding test data to serve as a check on the reasonableness of the model's results.

While FE model results have been compared to test measurements for each of the tests summarized in Table 1, there are currently no requirements or formal guidelines on which specific quantities of interest should be compared, or what measurable level of agreement would be acceptable demonstration of model validation. This paper focuses its discussion on four recent DOT-113 side impact tests and companion FE analyses [7, 8, 9, 10].

2. SIDE IMPACT SCENARIO

Figure 2 shows the tank car side impact test setup from the most recent DOT-113 test (Test 13). For the test, a standardized, repeatable, controllable, and safe impact scenario was chosen. The tank car undergoing testing is removed from its trucks (bogies) and placed on two skids intended to limit the amount of roll that can occur after impact. The tank car is then placed perpendicular to a set of railroad tracks, with the area of the shell

(i.e., cylindrical portion of the tank) to be impacted centered between the rails. The tank car is placed against a stiff wall, limiting its ability to move away from the impacting car. A heavy ram car, equipped with the desired impact head, is pulled back up a track with a descending grade that ends at the rigid wall. Based on the desired test impact speed, the ram car is released from an appropriate distance up this track. The ram car accelerates under gravity, ideally reaching the desired impact speed at the instant of contact between the end of the impact head and the shell of the tank car being tested. Table 1 provides a summary of each full-scale side impact test but does not explain all the details that differed from test- to-test.

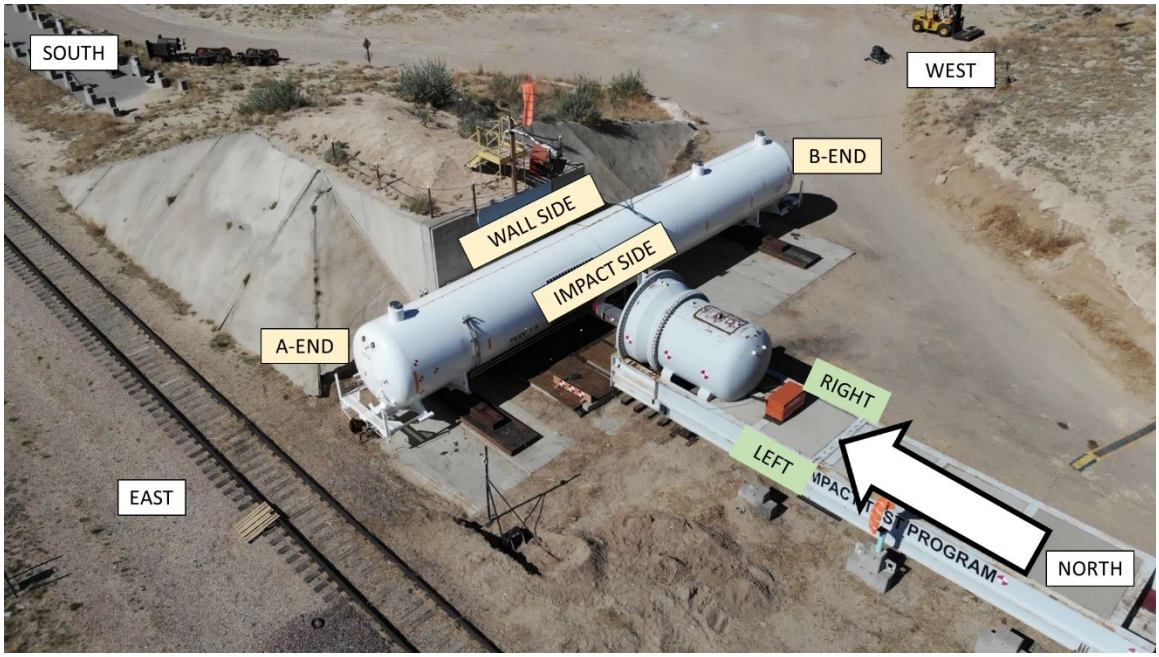

Figure 2. DOT-113 Side Impact Test Setup (Test 13 Shown)

2.1 Test Instrumentation

The instrumentation setup can vary slightly from test-to-test, depending on the details of the test, the tank car being tested, and the desired measurements. In general, each test includes instrumentation on both the initially-moving ram car and the initially-standing tank car. Tape switches are installed on the surface of the impact head and in the contact zone on the tank itself to allow the data acquisition systems on the ram car and the struck tank car to be synchronized to the time of impact.

The instrumentation used in the DOT-113 tests are summarized in Table 2. Many of the changes in instrumentation from Test 10 to 13 were made to accommodate testing with LN2/GN2 as opposed to water/air. Researchers acquired the test data using GMH Engineering Data BRICK Model III units. The data was anti-alias filtered at 1,735 Hz then sampled and recorded at a frequency of 12,800 Hz.

Table 2. Instrumentation Summary

Type of Instrumentation	Channel Count			
	Test 10	Test 11	Test 12	Test 13
Accelerometers	11	11	11	11
Speed Sensors	2	2	2	2
Pressure Transducers	8	13	5	4
String Potentiometers	4	10	4	4
Laser Displacement Transducers	0	15	15	15
Thermocouples	0	0	5	6
Temperature Probes	0	0	5	3
Total Data Channels	40	51	47	45

In addition to the measurements from the test instrumentation, one of the most readily apparent results of the test is whether the tank car punctured or resisted the impact without puncturing. This behavior, as well as the measured test data, are all candidates for inclusion in a procedure for model validation. Details of the instrumentation used in the impact tests is described in detail in the tank car side impact test reports [7, 8, 9, 10].

3. FINITE ELEMENT ANALYSIS

Previous work by Tang et al. [12] focused on verification of FEA on tank car side impacts using Abaqus/Explicit [13] and LS-DYNA [14] commercial FE programs. In this study, Abaqus/Explicit [11] was used to simulate the side impact tests.

This impact problem presents several challenges to simulation, each of which will affect the ultimate performance of the FE model and its suitability to simulate further impact conditions. The tank car side impact problem involves a dynamic impact with contact that evolves as the tank deforms. The tank car side will undergo elastic and plastic deformations, necessitating a material model for the steel that can adequately capture both behaviors. The model must also be capable of determining if puncture is likely to occur and if so, implementing a physically realistic numerical representation of material failure. For tests involving cryogenic liquids within the tank car, the material behaviors of the steel in contact with the LN2/GN2 must be appropriate for the corresponding cryogenic temperature. The tested cars featured fluid-structure interactions between the tank shell and two different fluid species, lading (water or LN2) and outage (air or GN2). The outage volumes in the FE models for Tests 10, 11, 12, and 13 were 17.6%, 17.6%, 9%, and 3.5% respectively.

For each side impact test, the FE model included a combination of deformable and rigid parts. The impactor, backing wall, and skids were modeled as rigid bodies. The tank car and its two-phase contents were represented as deformable bodies. The overall setup is shown in Figure 3 for the Test 13 side impact FE model. The models used reduced integration rectangular shell elements (S4) for most of the inner and outer tank, with a patch of reduced integration solid brick elements (C3D8R) in the tank's impact zone, where puncture initiates. The solid elements in the inner tank were approximately 0.05 inches and the solid elements in the outer tank were approximately 0.08 inches. Shell-to-solid coupling constraints were defined at the interfaces between shell and solid elements in the tanks.

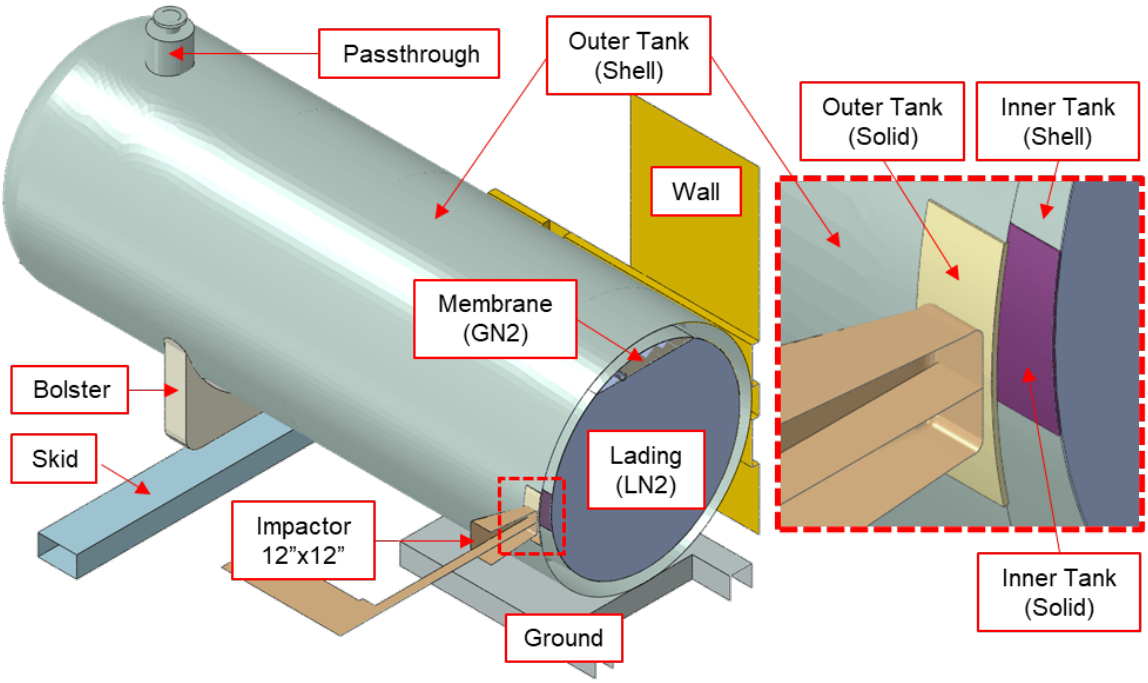

Figure 3. Annotated FE Model of DOT-113 from Test 13

Material behaviors must be defined within each model for the stainless steel inner tank, carbon steel outer tank, lading, and outage. Details on the approaches used to model the material behaviors of the various materials in the DOT-113 tank cars can be found in the respective test reports [7, 8, 9, 10]. Because both the strength and ductility of the steels can influence the puncture resistance of the tank car, understanding the material properties of the actual material of construction is an important aspect to consider in assessing the validity of a particular tank car model.

3.1 Validation of Finite Element Models

In previous papers presented at the ASME V&V Symposia in 2018 and 2020, the authors discussed various FE model validation methodologies applied to impact simulations [2] and applied two different validation methodologies to side impact simulations of a DOT-105 tank car and a DOT-117 tank car [3]. The current work applies the standardized methodology in ISO/TS 18571:2014 using CORA to compare FE results with test data in four recent DOT-113 side impact tests.

3.1.1 Validation Methodology

In this paper, the true curve (test data) is T and the CAE curve (FEA result) is C. For pre-processing, the FE results and test data were resampled by linear interpolation so that they had the same time step (Δt) of $7.8125 \cdot 10^{-5}$ s (12,800 Hz). No pre-processing was done to time-shift or scale the signals. Accelerometer data were filtered by a CFC-60 filter per SAE J211-1 [15].

CORA (ISO/TS 18571:2014)

ISO/TS 18571:2014 specifies a procedure for comparing FEA and test results using an overall score (R) consisting of:

(1) Phase (E_P)
(2) Magnitude (E_M)
(3) Slope or Shape (E_S)
(4) Corridor Score (Z)

Table 3 shows the ISO/TS 18571:2014 standardized constants that are specified in a configuration file when running the CORA software.

Table 3. ISO/TS 18571:2014 Constants for CORA

Corridor			Phase		Magnitude		Slope	
a_0	b_0	k_z	k_P	ε_P^*	k_M	ε_M^*	k_S	ε_S^*
0.05	0.5	2	1	0.2	1	0.5	1	2.0

ISO/TS 18571:2014 limits the metric to non-ambiguous signals, e.g., time-history curves. The metric has been previously applied to time-history signals from channel types such as force, moment, acceleration, velocity, and displacement. While CORA can average multiple test signals (repeated tests), the metric should only be applied to a single test-FEA pair.

3.1.2 Phase Score

The objective of a phase score is to quantify the phase shift between the test data and FEA result. In CORA, the phase score E_P is calculated by iteratively time-shifting the FEA result to the left and right by the time step Δt up to the maximum allowable fraction ε_P^* of the total time length. At each time-shift increment, the zero-normalized cross-correlation (ZNCC) of the two signals is computed. The term *zero* means that the mean of each signal is subtracted, and the term *normalized* means that the cross-correlation is divided by the standard deviation of each signal.

The number of increments needed to shift the FEA result to maximize the ZNCC is termed n_ε, and n is the total number of data points in the truncated curves. If n_ε is 0 then the phase score is perfect ($E_P = 1$); however, if it is greater than or equal to the maximum allowable increment shift ($\varepsilon_P^* \cdot n$) then the score is 0. In between 0 and the maximum allowable time-shift, the score scales linearly.

3.1.3 Magnitude Score

The objective of a magnitude score is to compare the relative amplitudes of the test data and FEA result. CORA's magnitude score E_M is computed by comparing the signals after performing dynamic time warping (DTW) on the optimally time-shifted FEA result (as described in Section 3.2.1 Phase Score). DTW is an algorithm used to compare the amplitudes of temporal signals that might have varying rates or pauses. A well-known application of DTW is in speech recognition, where different speakers typically have different speaking rates, pauses, etc. making it difficult to directly compare a spoken word with words in a database even when the word is clearly spoken [15]. In CORA's implementation, DTW is governed by a set of rules where:

- Every time point from the FEA result is matched with one or more time points from the test data, and vice versa.
- The first time point from the FEA result is matched to the first time point from the test result but it can also be matched with subsequent time points, and vice versa.
- The last time point from the FEA result is matched with the last time point from the truncated test data, but it can also be matched with prior time points, and vice versa, and;
- The time points for both signals must be monotonically increasing but each time step can individually expand or contract, i.e., dynamic warping.

Figure 4 shows a schematic example of DTW in CORA using the acceleration time-history signals from Test 13. The red curve is the FE result which has been first time shifted to maximize the phase score E_P and then time warped. The black curve is the test data which has been truncated to match the length of the FE result and then time warped. Time dilation is clearly visible as flat responses in the red and black curves and is annotated on the curves.

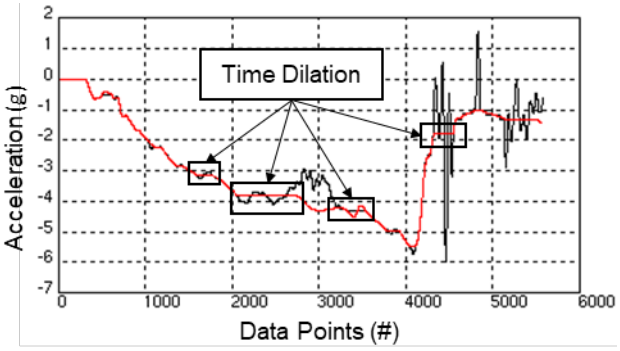

Figure 4. Example of Dynamic Time Warping using Test 13 Acceleration Time-History (CFC-60)

CORA's magnitude error ε_{mag} is calculated on the signals after DTW (C_i^{DTW} and T_i^{DTW}) using Equation (3).

$$\varepsilon_{mag} = \frac{\sum_{i=1}^{n} \left| C_i^{DTW} - T_i^{DTW} \right|}{\sum_{i=1}^{n} \left| T_i^{DTW} \right|} \qquad (1)$$

The magnitude score E_M is calculated by linearly normalizing ε_{mag} to the maximum allowable magnitude error $\varepsilon_M^* = 0.5$. This means that if on average the FEA result is off by 50% or more after DTW then it gets a score of $E_M = 0$. Conversely, if ε_{mag} is 0 then the magnitude score is a perfect $E_M = 1$.

3.1.4 Slope (Shape) Score

The objective of the slope score is to quantify the level of agreement in the overall shapes of the test data and FEA result. In CORA, the slope is compared by decimating (down-sampling) both signals by a factor of 10 to remove high frequency noise. It is important to note that *ISO/TS 18571:2014* recommends a sampling rate of 10kHz with a CFC-60 filter for acceleration data; this results in a 1 ms time step after decimation and a 100 Hz 3-dB limit frequency. The slopes of each curve are then calculated using a forward difference approximation with the

new time step. The slope percent error ε_{slope} is computed with respect to the slope of the test data at each new time point.

The slope percent error is then averaged and linearly scaled/scored, as previously discussed for phase and magnitude, according to the threshold ε_S^* of 200%.

3.1.5 Corridor Score

The objective of the corridor score is to compare the test data and FEA result on a point-to-point basis. The corridor score compares the curves at each time step, and because of this, it is extremely sensitive to distortions in phase (timing) between the signals, i.e., a minor distortion in phase can result in a very poor rating for these metrics.

In CORA, inner and outer corridors are defined by shifting the test data vertically by $\pm a_0 \cdot T_{norm}$ and $\pm b_0 \cdot T_{norm}$ respectively. At each time point, the signal receives a score of 1 if it is within the inner corridor and a score of 0 if it is outside the outer corridor. If it is between inner and outer corridors, then the score is calculated as a normalized quadratic function between the two corridors. The corridor score is then calculated as the average over the data points in the interval of evaluation.

3.1.6 Overall (Composite) Score

In CORA, the overall score R is calculated as a weighted sum of the corridor Z, phase E_P, magnitude E_M, and slope E_S scores using Equation (2) with the weights previously shown in Table 3.

$$R = w_Z \cdot Z + w_P \cdot E_P + w_M \cdot E_M + w_S \cdot E_S \qquad (2)$$

The overall score R is then used to determine a rating of *excellent*, *good*, *fair*, or *poor* where 1 is a perfect score and 0 is the worst possible score. Table 4 gives the minimum thresholds for each rating category.

Table 4. ISO/TS 18571:2014 Minimum Scores for CORA Ratings

Excellent	Good	Fair	Poor
0.94	0.80	0.58	0

3.2 CORA Validation Results

Table 5 summarizes the validation results for the analyses of the DOT-113 tests. For ease of comparison, the tables are color coded so that green corresponds to a perfect score (CORA=1) and red corresponds to a minimum score (CORA=0). In Tests 12 and 13, the authors were uncertain of the exact outage within the tank car due to technical difficulties in measuring the temperature, pressure, and weight of the two-phase cryogenic fluids within the car. The authors modeled the outage at 9% in Test 12 and 3.5% in Test 13 based on their best estimate using the pressure and temperature measurements taken prior to the test.

Table 5. DOT-113 CORA (ISO/TS 18571:2014) Overall Scores

Signals	Test 10	Test 11	Test 12	Test 13
Impactor Acceleration	0.532	0.854	0.875	0.605
Change in Air Pressure	0.906	0.808	0.722	0.606
String Pot Skid A-End	0.798	0.83	0.719	0.867
String Pot Skid B-End	0.473	0.806	0.846	0.534
String Pot Head A-End	0.904	†	0.809	0.931
String Pot Head B-End	0.744	†	0.885	0.527
Impactor Displacement	0.933	0.904	0.997	0.900
Average	0.756	0.840	0.836	0.710

† String potentiometer detached during test

Figure 5, Figure 6, Figure 7, and Figure 8 show the acceleration time-histories for Tests 10, 11, 12, and 13, respectively, in black. The corresponding FEA is shown in red, and the overall CORA score for the signal is annotated in each figure. For Test 10, which resulted in puncture of the outer and inner tanks, the authors calculated the CORA scores (i.e., interval of evaluation) up to the point where the FEA terminated due to numerical instability (0.204 seconds).

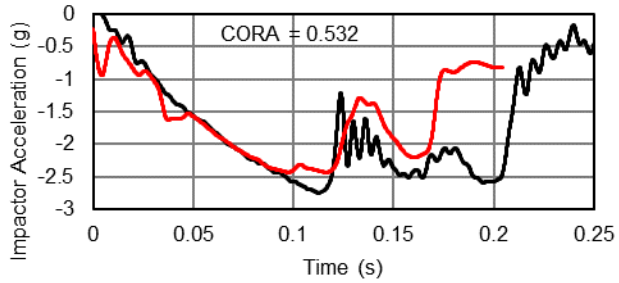

Figure 5. Test 10 Impactor Acceleration (CFC-60)

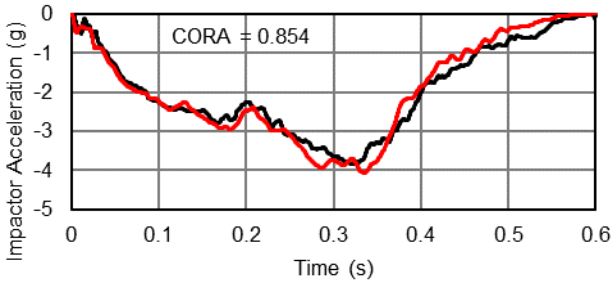

Figure 6. Test 11 Impactor Acceleration (CFC-60)

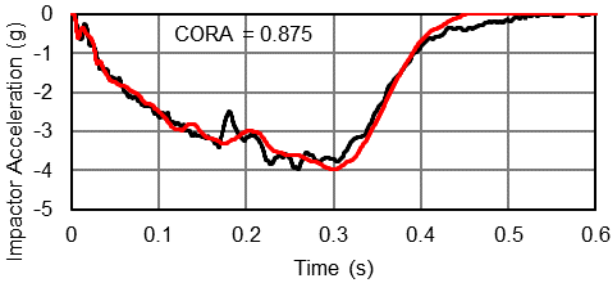

Figure 7. Test 12 Impactor Acceleration (CFC-60)

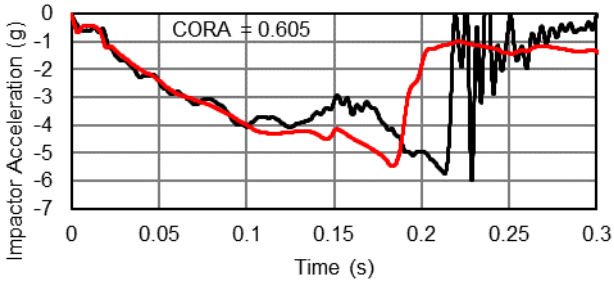

Figure 8. Test 13 Impactor Acceleration (CFC-60)

The CORA ratings were *poor* and *fair* for the impactor accelerations from Tests 10 and 13. These tests resulted in puncture of the tank car. The CORA ratings were *good* for the tests that did not result in puncture (Tests 11 and 12). Each test's corresponding FE model agreed with the puncture or non-puncture outcome of that test. The early termination of the FEA models made it difficult for CORA's automated preprocessor to properly time-shift the signals. Unfortunately, the automated time-shifting could not be disabled using the CORA configuration file. However, the authors found that running the simulation for a brief time prior to impact (e.g., -0.05s) could help with the automated time-shifting.

Figure 9, Figure 10, Figure 11, and Figure 12 show the change in outage pressure time-histories for the tests in black and corresponding FEA in red with the CORA scores annotated. To calculate the change in outage pressure, the authors subtracted the outage pressure at time equal to 0 seconds from the outage pressure signal, i.e., the outage pressure was offset.

In Figure 12, the authors observed a pressure spike in the Test 13 outage pressure that was not captured by the model. The authors have proposed two possible explanations for the observed pressure spike in Test 13: (1) the LN2 level rose to the top of the inner tank resulting in localized pressure spikes around the pressure transducers or (2) the LN2 underwent flash vaporization after puncture of the inner tank. The possibility of flash vaporization of LN2 after puncture is discussed in the Test 12 report [10].

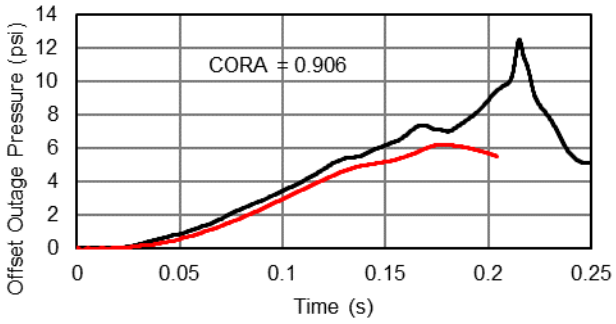

Figure 9. Test 10 Offset Outage Pressure

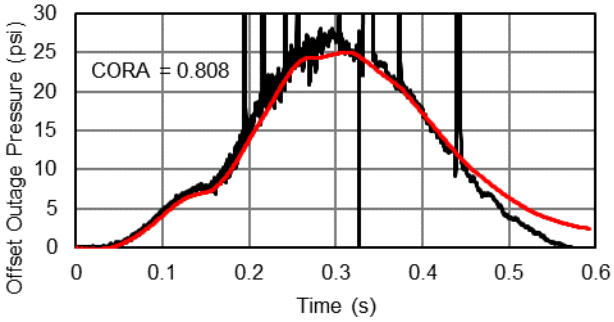

Figure 10. Test 11 Offset Outage Pressure

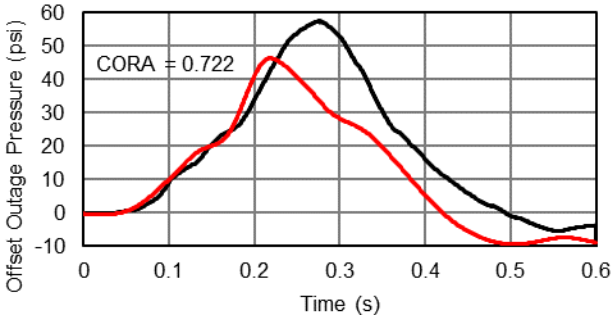

Figure 11. Test 12 Offset Outage Pressure

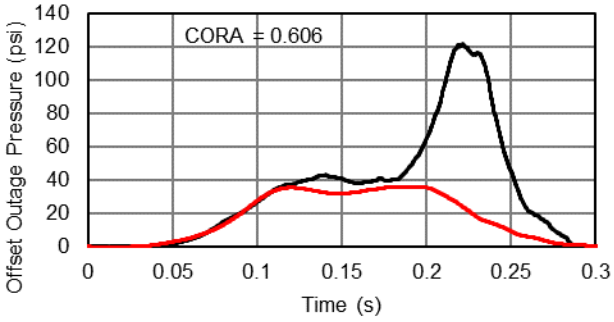

Figure 12. Test 13 Offset Outage Pressure

The FEA from Tests 10 and 11 with water/air achieved CORA ratings of *good* because: (1) the test outage pressure measurements were more accurate near room temperature, and (2) it is less complicated to model a room temperature gas because it can be modeled as an ideal gas. It is noteworthy, that the signal noise in the outage pressure signal in Test 11 (Figure 10) resulted in a lower CORA score for slope which uses a first-order differential and therefore amplifies the effect of noise. Additionally, the signal noise also affected the values for the corridor and magnitude scores.

The CORA rating was *fair* for Test 12 with LN2/GN2 which did not result in puncture; however, it should also be noted that there were large discrepancies in the multiple pressure transducers that measured the outage pressure during Test 12. The authors do not think the averaged signal represents the true outage pressure for Test 12.

Lastly, the CORA rating was *good* for Test 13 with LN2/GN2 which resulted in puncture. The authors were able to achieve more accurate measurements from the pressure transducers in this test; however, there was still an unrealistically high pressure spike after 0.18s that the authors attribute to the

liquid level rising to the top of the inner tank resulting in localized pressure buildup around the pressure transducers.

Figure 13, Figure 14, Figure 15, and Figure 16 show the impactor displacement time-histories for the tests in black and corresponding FEA in red with the CORA scores annotated. The CORA ratings were *good* or *excellent* for all the tests. However, the CORA interval of evaluation for Test 13 was truncated up to 0.25s due to a data spike which occurred after puncture possibly due to pressurized release of fluid from the inner tank obscuring the laser-based displacement transducers.

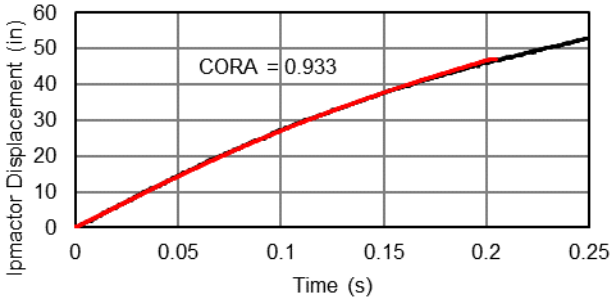

Figure 13. Test 10 Impactor Displacement

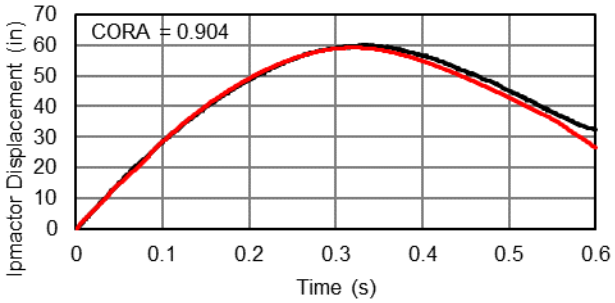

Figure 14. Test 11 Impactor Displacement

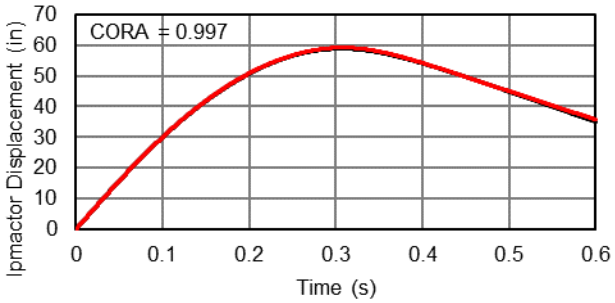

Figure 15. Test 12 Impactor Displacement

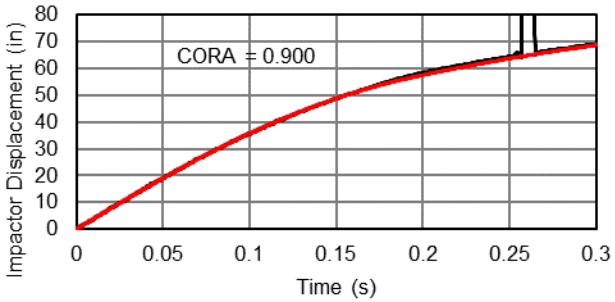

Figure 16. Test 13 Impactor Displacement

3.3 Interval of Evaluation

The DOT-113 side impact tests that did not result in puncture (Tests 11 and 12) did not require manual settings for the CORA interval of evaluation and were able to follow the procedures in ISO/TS 18571:2014. However, the DOT-113 side impact tests that did result in puncture (Tests 10 and 13) required manual settings for the CORA interval of evaluation for some of the signals to help correct the automated preprocessor time-shifting of the FEA results. This constitutes a deviation from the procedure in ISO/TS 18571:2014.

To study the effect of manually setting the interval of evaluation on the overall CORA score, the authors manually defined the interval of evaluation to end at different time points (t_{end}) in increments of 0.05s for Tests 10 and 13. Tests 11 and 12 were not included because the interval of evaluation could be calculated automatically per ISO/TS 18571:2014. Table 6 shows the overall CORA scores versus t_{end}, and the authors note that the overall CORA score was generally not sensitive to t_{end} after it reached 0.1s or greater.

Table 6. DOT-113 CORA Scores vs Interval of Evaluation

	CORA Overall Score	
t_{end}	Test 10	Test 13
0.05	0.636	0.542
0.1	0.731	0.722
0.15	0.744	0.74
0.2	0.758	0.736
0.25	†	0.736

† Test 10 simulation self-terminated before 0.25s

The lack of sensitivity of the overall CORA score to t_{end} indicates that the overall scores reported in Table 5 for Tests 10 and 13 would not vary excessively if a user of CORA were to manual set a different t_{end} for the interval of evaluation. If there were a large variation in overall CORA score for each increment of t_{end}, then the process of setting t_{end} would need more careful consideration and an automated process would be strongly preferred to prevent potential inflation of scores by tuning the interval of evaluation.

4. DISCUSSION

This section contains a discussion on signal selection, energy metrics, fluid response, and puncture/non-puncture outcomes.

4.1 Signal Selection

The authors selected the acceleration and displacement of the impactor, the offset outage pressure, and 4 external string pots attached to the tank car to conduct the validation exercise for tank car side impact model. Tests 11-13 each featured 4 pairs of laser displacement transducers that measured the deformation of the outer tank. Lastly, Test 11 featured 6 internal string pots that measured the deformation of the inner tank. These additional data channels could also be used for model validation, but they would tend to inflate the overall CORA score when using an unweighted average. For example, if all the functioning laser

transducers and string pots were included in the average CORA score for Test 11 it would increase from 0.840 (Table 5) to 0.885.

More thought should be given to creating a weighted average score for the tank car side impact model. For example, the authors consider the score for impactor acceleration to be more important than the displacement of one of the tank car skids since the magnitude of displacement of the tank car skid is relatively small due to the large length of the tank car, and the displacement of the skid can be greatly affected by friction between skid and ground. If only impactor accelerations were considered for the CORA ratings, then the overall rating for Test 10 would have changed from *fair* to *poor* while the other tests remained unchanged.

The authors also note that the CORA validation metrics for corridor, magnitude, and slope can be sensitive to signal noise. In this study, the signal noise in the offset outage pressure in Test 11 was significant, but the authors did not exclude it from the average CORA score because it did not appear to be an outlier. If the outage pressure would have been excluded, the average score from Test 11 would have increased from 0.840 (Table 5) to 0.849.

4.2 Energy Metrics

At the instant of impact, the kinetic energy of the initially-moving ram can be readily calculated using the velocity of the impactor and its mass. The energy imparted to the tank can be determined by first calculating the force-indentation response from the acceleration- and indentation-time histories for the ram car, and then numerically integrating the force-displacement response. As described in EN 15227:2020 [17], the energy absorbed during a dynamic impact is often a relevant result to be compared between test and analysis.

For the tank car side impact problem, the energy absorbed by the tank will either be equal to the initial kinetic energy (in the event of a non-puncture outcome) or will be less than the initial kinetic energy (if the tank punctures). The difference between the initial energy and the absorbed energy gives some indication of how close the speed of the impactor was to the critical threshold puncture speed; however, the relationship is non-linear and is complicated by fluid effects, e.g., sloshing.

The kinetic energy of the ram car could be considered as an additional signal for model validation; however, this signal would be derived from the impactor acceleration. If the impactor acceleration score is already included in the overall average, then it could be considered *double-counting* (i.e., including the same measurement twice in an average) to also include the impactor kinetic energy. One could also argue that including both impactor acceleration and displacement in the average could be considered *double-counting* because the impactor displacement could be accurately computed from the impactor acceleration, even though the measurements from the laser transducers were used to validate the impactor displacement.

4.3 Fluid Response

As demonstrated by the test results presented earlier in this paper, the fluid behavior inside the tank car can have a significant effect on the overall impact response of the tank car. One of the challenges associated with using test data to validate a model that will then be extrapolated to impact conditions beyond those tested is how valid the model remains as the conditions differ more significantly from what was tested. Modeling techniques that are appropriate to model one set of fluid conditions may not be equally suitable to model another set of fluid conditions. Significant changes to the impact setup, such as impactors of a different shape or size, may also influence the relative significance of the fluid behavior. A validation framework may need to consider the nature of the test and analysis initially used to validate the tank car side impact model and determine appropriate limits on the nature of the changes for which that model remains valid.

4.4 Puncture/Non-puncture Outcomes

During the impact test itself, one of the readily apparent outcomes is whether the tank has punctured, or if the tank resisted the impact without puncturing. If an FE model is used to simulate a test with the potential of a puncture outcome, the model must also be capable of simulating puncture. The quality of the puncture simulation will depend on such details as the availability of material coupons for testing, the ability of the failure/fracture behavior of the material to be characterized based upon those material tests, and the ability of the FE software to numerically implement the failure/fracture behavior.

Further, it may be appropriate to consider puncture not as a binary outcome, but to consider the character of the puncture in assessing the performance of the model. The *CORA* framework was not developed to specifically evaluate puncture as a mode of failure between a simulation and a test. Future work may be appropriate to consider including a specific qualitative and/or quantitative score to account for the puncture response as a specific feature of the tank car side impact scenario.

5. CONCLUDING REMARKS

FRA has sponsored a series of tests and corresponding FE analyses of side impacts tests of DOT-113 railroad tanks cars. While the test measurements have been compared with the results of corresponding FE models, specific model validation procedures have not yet been adopted for validating tank car side impact models. As a starting point at developing a model validation framework for tank car side impact tests, the authors utilized the ISO/TS 18571:2014 model validation procedure with CORA on selected time-history data signals from the impact tests and models. However, further work is necessary to adapt the ISO/TS 18571:2014 procedure to tank car side impact tests that result in puncture. Further consideration is needed for determining the interval evaluation for tests/simulations involving puncture, incorporating the puncture/non-puncture outcomes into the average CORA score, averaging CORA scores to compute an overall score, selecting threshold(s) for successful model validation, and providing guidelines for extrapolating a validated model to other impact conditions.

ACKNOWLEDGEMENTS

The testing described in this paper was performed by MxV at the Transportation Technology Center (TTC) in Pueblo, Colorado. Steve Belport, Shawn Trevithick, Travis Gorhum, and Nicholas Wilson lead the testing effort. The authors also wish to

acknowledge the contributions of Dr. David Jeong (retired) of the Volpe Center to the overall success of the tank car structural integrity research program.

REFERENCES

[1] Partnership for Dumy Technology and Biomechanics, "CORA," July 2023. [Online]. Available: https://www.pdb-org.com/en/information/18-cora-download.html.

[2] M. Carolan, B. Perlman and F. González III, "Validation of puncture simulations of railroad tank cars using full-scale impact test data," in *ASME Verification & Validation VVS2018-9322*, Minneapolis, MN, 2018.

[3] S. Eshraghi, M. Carolan, B. Perlman and F. González III, "Comparison of methodologies for finite element model validation of railroad tank car side impact tests," in *ASME Verification and Validation Symposium VVS2020-8822*, Virtual Online, 2020.

[4] R. H. Malcom and M. Mongiardini, "Roadside Safety Verification and Validation Program (RSVVP) User Manual," December 2008. [Online]. Available: https://roadsafellc.com/NCHRP22-24/QPR/AttachmentD-7.pdf.

[5] ISO/TS 18751:2014, "Road Vehicles - Objective Rating for Non-Ambiguous Signals".

[6] PHMSA, DOT, "Tank-head puncture-resistance systems.," 2015. [Online]. Available: https://www.govinfo.gov/content/pkg/CFR-2015-title49-vol3/pdf/CFR-2015-title49-vol3-sec179-16.pdf.

[7] PHMSA, DOT, "Performance standard requirements (DOT-117P)," 2015. [Online]. Available: https://www.govinfo.gov/content/pkg/CFR-2019-title49-vol3/pdf/CFR-2019-title49-vol3-sec179-202-12.pdf.

[8] S. Trevithick, M. Carolan, S. Eshraghi and N. Wilson, "Side Impact Test and Analyses of a Legacy DOT 113 Tank Car," U.S. Department of Transportation DOT/FRA/ORD-21/28, Washington, D.C., September 2021.

[9] N. Wilson, M. Carolan, S. Trevithick and S. Eshraghi, "Side Impact Test and Analyses of a DOT-113 Surrogate Tank Car with Water," U.S. Department of Transportation, DOT/FRA/ORD-21/35, 2021.

[10] S. Belport, M. Carolan, S. Trevithick, S. Eshraghi and A. Krishnamurthy, "Side Impact Test and Analyses of a DOT-113 Surrogate Tank Car Filled with Cyrogenic Lading," U.S. Department of Transportation, DOT/FRA/ORD-22/33, Washington, D.C., September 2022.

[11] Federal Railroad Administration, "Full-Scale Shell Impact Test of a DOT-113C120W9 Tank Car Filled with Liquid Nitrogen - RR 22-10," July 2022. [Online]. Available: https://railroads.dot.gov/elibrary/full-scale-shell-impact-test-dot-113c120w9-tank-car-filled-liquid-nitrogen.

[12] Y. Tang, H. Yu, J. Gordon and D. Jeong, "Analysis of railroad tank car shell impacts using finite element method," in *Joint Rail Conference, JRC2008-63014*, 2008.

[13] Dassault Systèmes, Abaqus/Explicit User's Manual, Version 2019.

[14] Livermore Software Technology Corporation (LSTC), "LS-DYNA (R) Theory Manual," 24 July 2019. [Online]. Available: https://ftp.lstc.com/anonymous/outgoing/jday/manuals/DRAFT_Theory.pdf.

[15] SAE, "Recommended Practice J211/1 - Instrumentation for Impact Test - Part 1 - Electronic Instrumentation, March 1995. Available Online: https://www.sae.org/standards/content/j211/1_199503/," March 1995. [Online]. Available: https://www.sae.org/standards/content/j211/1_199503/.

[16] L. Rabiner and B.-H. Juang, Fundamentals of speech recognition, N.J.: PTR Prentice Hall, 1993.

[17] EN 15227, "Railway Applications—Crashworthiness Requirements for Railway Vehicle Bodies," European Committee for Standardization, Brussels, 2020.